Sensors and Materials, Vol. 27, No. 6 (2015) 465–474
MYU Tokyo

S & M 1084

A Review of Nanotechnology for Highly Sensitive Photodetectors for Vision Sensors of Insect-like Robots

Woo-Ram Lee[1], Hyoungho Ko[2], Dong-il "Dan" Cho[1], Kyo-in Koo[3,*] and Jong-Mo Seo[1,4,**]

[1]Department of Electrical and Computer Engineering, Seoul National University, 1 Gwanak-ro, Gwanak-gu, Seoul 151-742, Korea
[2]Department of Electronics Engineering, Chungnam National University, 99 Daehak-ro, Yuseong-gu, Daejeon 305-764, Korea
[3]Department of Biomedical Engineering, University of Ulsan, 93 Daehak-ro, Nam-gu, Ulsan 680-749, Korea
[4]Seoul National University Hospital Biomedical Research Institute, Seoul National University Hospital, 101 Daehak-ro, Jongno-gu Seoul 110-744, Korea

(Received December 8, 2014; accepted April 28, 2015)

Key words: insect-like robots, quantum dots, nanowire, highly sensitive photodetector

Insect-like robots for various purposes have been widely studied in recent years. Owing to the small size of the insect-like robots, reducing the size of the receptive field is an important subject. Furthermore, most insect-like robots are required to work at night as well as day. Therefore, an ultrahigh-sensitivity sensor with an ultrasmall size is essential for the realization of insect-like robots. A high photon-to-electron conversion efficiency above the limitation of conventional devices can be achieved in a nanostructure owing to its quantum effect. In this paper, we report on the fabrication methods and materials for making nanostructures, and introduce nanostructure photodetectors with an explanation of the principle of the quantum effect.

1. Introduction

Robots are typically designed as autonomous machines to help humans.[(1)] There are many types of robot, from manufacturing machines to humanized robots. Recently, researchers have tried to make insect-like robots for various purposes, such as military and surveillance.[(2–4)] For example, in the military field, micro air vehicles (MAVs) have been developed for reconnaissance missions. MAVs are expected to replace surveillance cameras in the near future.[(5)]

*Corresponding author: e-mail: kikoo@ulsan.ac.kr
**Corresponding author: e-mail: callme@snu.ac.kr

ISSN 0914-4935

However, the development of the insect-like robot has a lot of problems concerning its practical usage. In particular, the vision sensor is one of the most critical issues. Owing to the tiny size of the insect-like robot, the receptive field of its vision sensor should decrease. Furthermore, despite its minimized size, it must work in dark environments. Therefore, an ultrahigh-sensitivity sensor with an ultrasmall size should be realized. The conventional photodetector has a limitation in terms of photosensitivity. Some solutions such as a silicon photomultiplier (SiPM), an avalanche photodiode (APD), and a hybrid photodiode (HPD) can increase photosensitivity dramatically and can count the number of photons.[6] Because of their high power consumption, they cannot be utilized for the insect-like robot. Recent brilliant progress in nanomaterials has induced vigorous research on ultrahigh-sensitivity photodetectors.[7–9] In this paper, we introduce nanotechnology principles for a highly sensitive photodetector and several implementations with its fabrication method and performance as the vision sensor of an insect-like robot.

2. Quantum Effect in Nanostructure

The maximum energy transfer efficiency from a photon to an electron in a single p-n junction was calculated as 31% by Shockley and Queisser, which is called the S-Q limit.[10] There are many approaches to making a solar cell with higher efficiency than the S-Q limit, such as a tandem cell, a hot carrier solar cell, or a multiband solar cell.[10–13] One of the good methods of achieving higher efficiency is multiple excitation generation (MEG) caused by impact ionization in the nanostructure.[10,14–18]

When a photon having larger energy than the bandgap is injected to a semiconductor, the photon transforms into extra holes and electrons. Excess energy above the bandgap is converted into kinetic energy of the electron. Electrons with high kinetic energy undergo impact ionization, which is a MEG process. A carrier with high energy can lose its energy into the conduction band accompanied by the generation of another electron from the valence band, as shown in Fig. 1. As a result, one photon makes two electron-hole

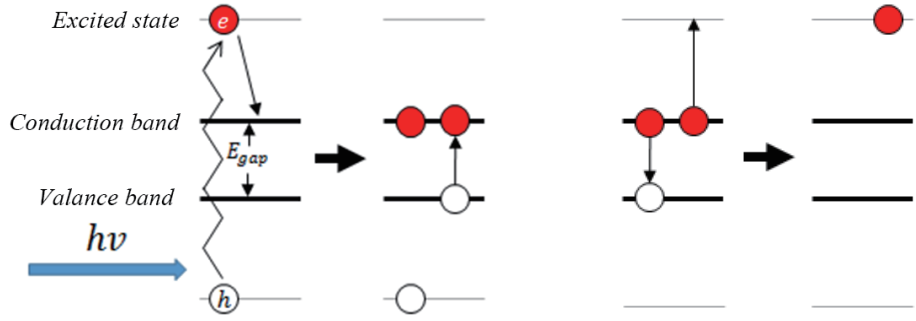

Fig. 1. (Color online) (a) Impact ionization and (b) Auger recombination.

pairs. However, electrons at the conduction band also undergo Auger recombination. Auger recombination is an inverse impact ionization in which an extra electron in the conduction band loses its energy by recombination with a hole in the valence band, followed by the emission of another electron in the same atom.[19] Therefore, the number of photoinduced electrons is reduced by Auger recombination.

If the nanostructure size is comparable to or smaller than the de Broglie wavelength, the recombination rate decreases dramatically.[10] Holes in the nanostructure are quickly removed by a fast hole trap at the surface since the nanostructure has a high surface-to-volume ratio. This fast hole trap phenomenon decreases the Auger recombination rate, because the number of holes dominates the Auger recombination rate. Eventually, the impact ionization rate can be competitive with the Auger recombination rate. In other words, the minority carrier lifetime increases.[14] This phenomenon is observed in CdSe.[20]

Nanowires have a high photon-to-electron conversion efficiency affected by the above-mentioned mechanism as well. When the different workfuction media meet each other, charges are redistributed to equalize the Fermi level. The energy band is bent at the surface of the semiconductor. This is called the Fermi energy level pinning effect. Because of the Fermi energy level pinning effect and high surface-to-volume ratio, a nanowire has vast depletion layers. The depletion layer can separate holes and electrons physically. If holes and electrons are physically separated, the carrier's lifetime is increased.[21] When the nanowire diameter is under a certain critical length, the nanowire becomes fully depleted. Therefore, by following Lingquan's simulation, photoinduced conductivity is twelve times higher than that of a bulk semiconductor in the illumination state.[21] Furthermore, the simulation shows that the fully depleted nanowire has a very low conductivity in the dark state, which shows an extremely low thermal noise level. Consequently, a nanowire photodetector can exhibit a high illuminated-to-dark conductivity ratio, which is an important property of highly sensitive photodetectors.

3. Fabrication of Nanostructure

Top-down and bottom-up approaches are the two major strategies of nanostructure fabrication. In this section, nanoimprint lithography and the size reduction method by chemical reaction will be reviewed for the top-down approaches. For the bottom-up approaches, direct-growth and transfer printing will be introduced.

3.1 *Nanoimprint lithography*

One of the famous top-down approaches is e-beam lithography (EBL). The resolution of EBL can be sub-10 nm.[22] However, it suffers from low throughput and high cost. Nanoimprint photolithography is a promising solution for low-cost and high-throughout fabrication while retaining the merits of EBL. A patterned wafer made by EBL is used as an imprint mold. A thin layer of resist, which can be cured by UV or heat, is spin-coated on a substrate. Sequentially, the mold is pressed on the resist layer. After applying UV or heat, the mold is detached. The residual layer is cleaned by anistropic wet or plasma etching. Spotless and inverted nanopatterns can be produced by simple stamping. Furthermore, the mold can be reused. Morton *et al.* demonstrated

a wafer-scale pattern of a sub-40-nm vertical silicon nanowire with a high aspect ratio using nanoimprint lithography, as shown in Fig. 2(a).[23] Using the Cr layer additionally, they achieved a vertical nanowire array of 50 nm diameter, which has an aspect ratio of up to 60:1.

3.2 *Size reduction by chemical reaction*

By changing a substrate into another material by chemical reaction, a nanostructure can be produced. The suspended silicon nanowire connections with sub-100-nm diameter demonstrated by Lee *et al.* are a good example, as shown in Fig. 2(b).[24] They used anisotropic wet etching and silicon thermal oxidation. Nanowires of 100 nm diameter were created by reducing a 1 μm oxide line pattern on a silicon substrate. The oxide pattern was made using a stepper. After patterning a 1 μm oxide line, deep reactive ion etching (DRIE) was carried out. Then, the silicon substrate was etched using a tetramethylammonium hydroxide (TMAH) solution to make anisotropic structures. After being etched by TMAH, the cross section of the line looks like a sandglass. Subsequently, the silicon line that looks like a sandglass is changed into silicon oxide by wet oxidation; therefore, the silicon line becomes thinner. After the removal of silicon oxide using an HF-based solution, suspended silicon nanowire bridges are revealed.[24]

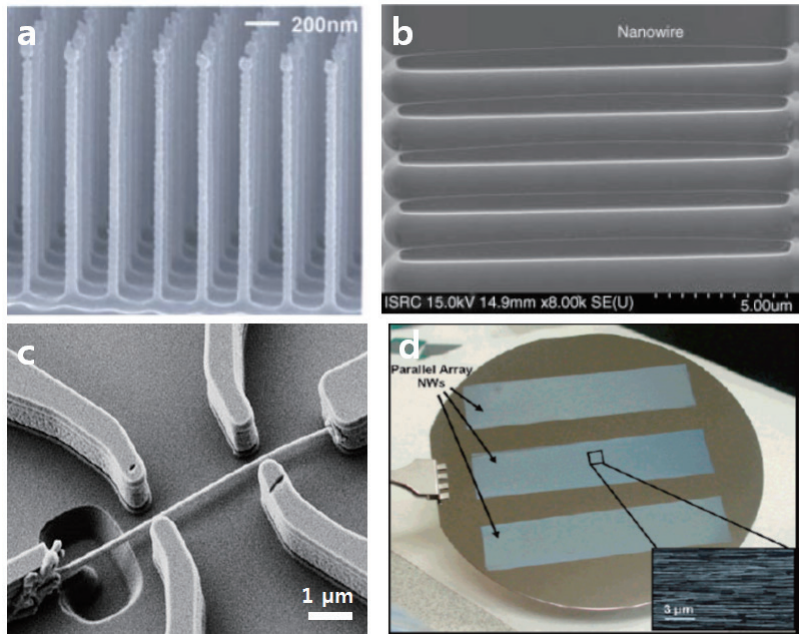

Fig. 2. (Color online) (a) Nanowire pillar array formed by nanoimprint lithography.[23] (b) Suspended silicon nanowire array formed by size reduction using chemical reaction.[24] (c) Nanowire bridge made by VLS method.[27] (d) Wafer-scale Ge nanowire arrays on the Si/SiO_2 wafer formed by contact printing.[33]

3.3 *Direct growth*

The vapor-liquid-solid (VLS) mechanism is a fabrication method using an epitaxy process for a one-dimensional structure such as a nanowire. This mechanism can control the location and diameter by patterning metal catalysts. Nanowires produced by the VLS process are crystalline with a free standing capability.[25] The process of the VLS mechanism is as follows: First, metal catalysts are patterned where the nanowire will grow. The prepatterned metal catalysts change into liquid beads at high temperature. When the vaporized precursor element meets the alloy, it becomes supersaturated. Excess elements are precipitated, and crystal growth subsequently occurs at the alloy-substrate interface. One of the advantages of the VLS mechanism is that horizontal nanowire growth at the side wall is possible.[26] Well-ordered horizontal nanowire bridges with selective positioning were demonstrated by Fernandez-Regules *et al.*, as shown in Fig. 2(c).[27] Au nanoparticles are deposited selectively on the Si surface via the SiO_2 surface. A specific structure on the silicon-on-insulator (SOI) wafer is made by photolithography and DRIE. After the oxidation, the SiO_2 layer is etched to expose the Si vertical surface where the nanowire will grow. Sequentially, Au nanoparticles are deposited. By the VLS method, horizontal nanowire growth occurs at the vertical surface only where the oxide was cleared away.

Molecular beam epitaxy (MBE) is a method of depositing a monocrystalline film. It was invented by Cho and Arthur in the 1970s.[28] Solid gallium or arsenic is sublimated by heat in separate quasi-Knudsen effusion cells. Before the gaseous precursor element reaches the substrate, it does not react with any other gases because it has a long mean free path. MBE has a very low deposition rate (under 1000 nm/min). Therefore, an ultrahigh vacuum is required. MBE can make a smooth growth surface with steps of atomic height. An IR photodetector with quantum dots (QDs) in a well (DWELL) is demonstrated by the Center for High Technology Materials (CHTM).[29] Self-organized InAs/InGaAs QD arrays on the GaAs substrate are grown in a V-80 MBE.

3.4 *Transfer printing*

The substrate material could be restricted by the fabrication method. For example, a plastic substrate cannot be used for silicon nanowire epitaxy because high temperature is required. In contrast, transfer printing can use any type of substrate with good properties such as biocompatibility, flexibility, or transparency.[30] After making the nanowires on the mother plate, they are harvested by various methods. The harvested nanowires are transferred onto a good target plate. Transfer printing can be categorized as dry transfer,[31] wet transfer,[32] or contact printing.[33]

4. Materials for Nanostructure Photodetector

4.1 *Carbon family: silicon and carbon nanotubes*

Si and Ge are broadly used in photodetectors because their fabrication process and properties have been well studied.[34] Si is naturally an indirect-bandgap semiconductor. If the momentum of the maximal energy state in the valence band is the same as the momentum of the minimal energy state in the valence band, it is called a direct bandgap.

Otherwise, it is an indirect bandgap. However, silicon nanowire arrays can have a direct bandgap if they are grown toward the crystallographic orientation.[35] Astonishingly, we can modify the silicon nanowire bandgap by controlling the wire diameter with surface passivation agents.[36] Physical and optical properties of semiconductor materials are shown in Table 1. H, OH, NH_2, and halogens can be used for surface terminations.[37] However, the tolerances of the wire diameter are within 1–3 nm. Carbon nanotubes (CNT) are wonderful materials for IR detectors because of their exceptional optical and electrical properties.[38] A single-walled carbon nanotube (SWNT) thin film can absorb a broad wavelength from the UV to the far-IR region.[39] The absorption rate of the incident radiation reaches over 70% in a 100-nm-thick film.[40] Moreover, a CNT IR detector can exhibit high quantum efficiency without temperature cooling, unlike other commercial IR detectors.[38]

4.2 *III-V compounds*

The advantages of group III-V compounds are their direct bandgap, high carrier mobility, and ease of doping.[34] The direct bandgap allows the photodetector to absorb light more efficiently. Wavelength sensitivity is also controllable by alloy bandgap engineering.[34] In the case of GaAs, fast nanowire growth can be possible on various substrates.[41] Recently, GaAs epitaxial growth on a graphene substrate has been reported by Munshi *et al.*[42] They achieved GaAs nanowire growth on graphene using a two-temperature growth strategy, which means that GaAs nanowires grow at two different temperatures. Ga droplets have a low contact angle at low temperature (540 °C). This enhances nanowire nucleation; however, parasitic crystals are also frequently created. To prevent the growth of parasitic crystals, a subsequent growth step is conducted at high temperature (610 °C). InAs nanowire growth on single-layer graphene has also been reported.[43] Group III nitrides are good compounds for UV photodetectors because of their high thermal stability, wide bandgap, high breakdown voltage, and high photoresponsivity.[44,45]

4.3 *Metal oxides*

The properties of metal-oxide one-dimensional nanostructures, such as bandgap, and photoresponsivity, have been widely studied for electrooptical devices.[46,47] There are many types of metal-oxide photodetector with various bandgaps (ZnO, SnO_2, Cu_2O, Fe_3O_4, In_2O_3, CdO, and CeO_2).[47] ZnO is an efficient material for UV detection. ZnO

Table 1
Physical and optical properties of semiconductor materials.

Material	Sensing light	Bandgap	Photoresponsivity (A/W)	Reference
Si nanowire	Visible, near IR	Tunable	$1–10^5$	8, 9, 35, 36
SWNT thin film	UV, far IR	Tunable	—	39, 53
GQD-like array	Visible, mid IR	Defect midgap states band	1–8.61	7
InAs nanowire	Visible, near IR	0.354 eV	$1–4.4\times10^3$	54
GaN nanowire	UV	3.4 eV	1–70.4	55
ZnO nanowire	UV	3.37 eV	1–640	56

nanowires show high resistivity above 3.5 MΩ·cm in darkness. In contrast, their resistivity is reduced by 4 to 6 orders of magnitude under exposure to UV light below 380 nm.[48] Therefore, ZnO nanowires show a low dark current and a high illuminated-to-dark conductivity ratio. Furthermore, ZnO materials can be used inside the living body because they are biocompatible.[49]

5. Realization of Nanostructure Photodetector

A highly sensitive graphene photodetector with high photoresponsivity was demonstrated by Zhang *et al.*, as shown in Fig. 3(a).[7] Graphene's carrier mobility is tremendously high.[7] It can absorb ~2.3% of light over a vast wavelength range.[50]

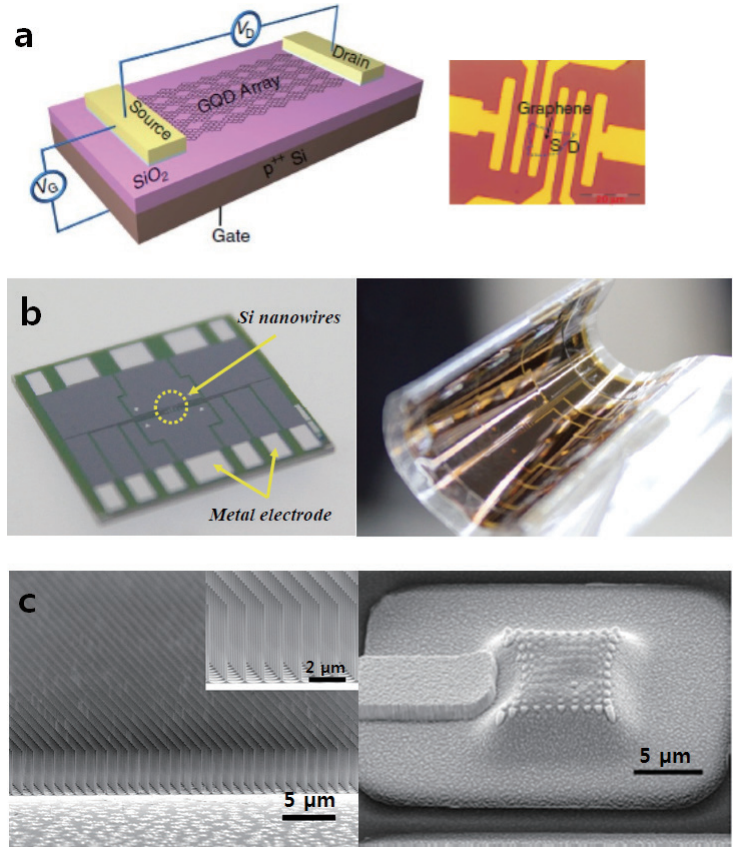

Fig. 3. (Color online) Examples of nanostructure photodetector. (a) Monolayer graphene photodetector with quantum-dot-like array.[7] (b) Silicon nanowire photodetector fabricated by size reduction method. The right image shows that the photodetector is made on a flexible substrate using polyimide.[8] (c) Photodetector with vertical silicon nanowire array.[9]

However, its photoresponsivity is relatively low in the case of pure graphene. There are many approaches for improving photoresponsivity, such as forming plasmon on the surface or implanting a microcavity; notwithstanding, graphene still exhibits low performance under 10 mA/W.[51,52] To achieve high photoresponsivity, Zhang *et al.* made a QD-like array on graphene, which shows a high photoresponsivity of 8.61A/W. To make a graphene QD (GQD)-like array, first of all, monolayer graphene is made on the SiO_2 substrate by mechanically exfoliating and transferring. Then, a thin Ti layer is deposited on the graphene using an e-beam evaporator. Finally, the Ti layer is removed via wet etching, so that the GQD array is fabricated. The size of QDs depends on the Ti layer thickness.

A silicon nanowire photodetector on a flexible substrate was demonstrated by our group, as shown in Fig. 3(b).[8] We fabricated a silicon nanowire by size reduction lithography, and transferred the silicon nanowire to a flexible substrate. We examined the optical properties of the photodetector between 0 and 4000 lux. As the light intensity increases, the photocurrent shows an exponential response, which can be good for low-light sensing. The photocurrent at the light intensity of 1.2 $\mu W/Cm^2$ is measured at 0.0833 μA, which means that the photodetector is extremely sensitive. The photoresponsivity is over 1×10^4 A/W.

Zhang *et al.* of the University of California devised a photodetector using a vertical silicon nanowire by nanoimprint lithography, as shown in Fig. 3(c).[9] Only 3% of the area of the photodetector is a receptive field. Nonetheless, it shows a high photoresponsivity under the condition of less than 0.1 $fw/\mu m^2$ incident power per nanowire. The device can detect IR light beyond 1560 nm. The photoresponsivity can reach 10^5 A/W for visible light and 10^2 A/W for IR light. However, the gain is saturated at about 170 K, and the dark current at a higher temperature becomes excessive.

6. Conclusions and Perspective

We have presented an overview of the nanotechnology for highly sensitive photodetectors. The quantum effect in a nanostructure makes the minority carrier lifetime longer. As a result, the number of photoinduced electrons is increased. Furthermore, a low dark current can be seen in the fully depleted region, which is formed by the Fermi level pinning effect at the surface. Therefore, a high illuminated-to-dark conductivity ratio can be realized. There are many types of fabrication method. Each fabrication method has pros and cons; thus, it should be carefully chosen in different situations. Currently, nanowire photodetectors have issues such as precise fabrication (diameter, doping concentration, uniformity, and orientation), CMOS circuit integration, reproducibility, and reliability. Although these issues make it difficult to commercialize one-dimensional or quasi-one-dimensional nanostructured photodetectors, we expect that nanostructured photodetectors will be the next-generation photodetectors in the near future.

Acknowledgements

This research was supported by a grant to BioMimetic Robot Research Center funded by the Defense Acquisition Program Administration (UD130070ID). This work was also supported by the Basic Science Research Program through the National Research Foundation of Korea (NRF) funded by the Ministry of Science, ICT & Future Planning (NRF-2014R1A1A1 038335).

References

1 The History of Robotics, http://www.redorbit.com/education/reference_library/technology_1/robotics-technology_1/1112942014/the-history-of-robotics/.
2 P. Shadbolt: Robo-Wings: Military Drones That Mimic Hawks and Insects, CNN, http://edition.cnn.com/2015/01/14/tech/mci-drone-robohawk-robofly/.
3 M. Hanlon: UAVs Get Smaller: The Micro Air Vehicle Nears Readiness, http://www.gizmag.com/go/4779/.
4 J. Peirs, J. Clijnen, D. Reynaerts, H. Van Brussel, P. Herijgers, B. Corteville and S. Boone: Sens. Actuators, A **115** (2004) 447.
5 D. J. Pines and F. Bohorquez: J. Aircr. **43** (2006) 290.
6 A. Rochas, H. Zbinden, N. Gisin, P. Eraerds and M. Legr: Opt. Express **15** (2007) 8237.
7 Y. Zhang, T. Liu, B. Meng, X. Li, G. Liang, X. Hu and Q. J. Wang: Nat. Commun. **4** (2013) 1811.
8 S. Lee, S. W. Jung, S. Park, J. Ahn, S. J. Hong, H. J. Yoo, M. H. Lee and D. I. Cho: Ultra-High Responsivity, Silicon Nanowire Photodetectors for Retinal Prosthesis (IEEE, Paris, 2012) pp. 1364–1367.
9. A. Zhang, H. Kim, J. Cheng and Y. Lo: Nano Lett. **10** (2010) 2117.
10 A. J. Nozik: Physica E **14** (2002) 115.
11 P. T. Landsberg, H. Nussbaumer and G. Willeke: J. Appl. Phys. **74** (1993) 1451.
12 S. Kolodinski, J. H. Werner, T. Wittchen and H. J. Queisser: Appl. Phys. Lett. **63** (1993) 2405.
13 A. Luque and A. Marti: Phys. Rev. Lett. **78** (1997) 5014.
14 A. J. Nozik: Annu. Rev. Phys. Chem. **52** (2001) 193.
15 D. S. Boudreaux, F. Williams and A. J. Nozik: J. Appl. Phys. **51** (1980) 2158.
16 H. Benisty, C. M. Sotomayor-Torres and C. Weisbuch: Phys. Rev. B **44** (1991) 10945.
17 U. Bockelmann and G. Bastard: Phys. Rev. B **42** (1990) 8947.
18 H. Benisty: Phys. Rev. B **51** (1995) 13281.
19 UPAC: Compendium of Chemical Terminology, 2nd ed. (1997).
20 P. Guyot-Sionnest, M. Shim, C. Matranga and M. Hines: Phys. Rev. B **60** (1999) R2181.
21 L. Wang and P. Asbeck: Analysis of Photoelectronic Response in Semiconductor Nanowires (Nanotechnology, IEEE-NANO, 2006) p. 716.
22 W. Hu, K. Sarveswaran, M. Lieberman and G. H. Bernstein: J. Vac. Sci. Technol. B **22** (2004) 1711.
23 K. J. Morton, G. Nieberg, S. Bai and S. Y. Chou: Nanotechnology **19** (2008) 345301.
24 K.-N. Lee, S.-W. Jung, K.-S. Shin, W.-H. Kim, M.-H. Lee and W.-K. Seong: Small **5** (2008) 642.
25 N. Wang, Y. Cai and R. Q. Zhang: Mater. Sci. Eng. R **60** (2008) 1.
26 M. S. Islam, S. Sharma, T. I. Kamins and R. S. Williams: Nanotechnology **15** (2004) L5.
27 M. Fernandez-Regulez, M. Sansa, M. Serra-Garcia, E. Gil-Santos, J. Tamayo, F. Perez-Murano and A. San Paulo: Nanotechnology **24** (2013) 7.

28 A. Y. Cho and J. R. Arthur: Prog. Solid State Chem. **10** (1975) 157.
29 A. V. Barve, S. J. Lee, S. K. Noh and S. Krishna: Laser Photonics Rev. **4** (2010) 738.
30 L. Vj, J. Oh, A. P. Nayak, A. M. Katzenmeyer, K. H. Gilchrist, S. Grego, N. P. Kobayashi, S.-Y. Wang, A. A. Talin, N. K. Dhar and M. S. Islam: IEEE J. Sel. Top. Quantum Electron. **17** (2011) 1002.
31 K. J. Lee, M. J. Motala, M. A. Meitl, W. R. Childs, E. Menard, A. K. Shim, J. A. Rogers and R. G. Nuzzo: Adv. Mater. **17** (2005) 2332.
32 M. G. Kang, J. H. Ahn, J. Lee, D. H. Hwang, H. T. Kim, J. S. Rieh, D. Whang, M. H. Son, D. Ahn, Y. S. Yu and S. W. Hwang: J. Appl. Phys. **49** (2010) 4.
33 Z. Y. Fan, J. C. Ho, Z. A. Jacobson, R. Yerushalmi, R. L. Alley, H. Razavi and A. Javey: Nano Lett. **8** (2008) 20.
34 C. Soci, A. Zhang, X. Y. Bao, H. Kim, Y. Lo and D. Wang: J. Nanosci. Nanotechnol. **10** (2010) 1.
35 M. Hasan, M. F. Huq and Z. H. Mahmood: SpringerPlus **2** (2013) 141.
36 M. Nolan, S. O'Callaghan, G. Fagas and J. C. Greer: Nano Lett. **7** (2007) 34.
37 P. W. Leu, B. Shan and K. Cho: Phys. Rev. B **73** (2006) 195320.
38 Q. Zeng, S. Wang, L. Yang, Z. Wang, T. Pei, Z. Zhang, L. M. Peng, W. Zhou, J. Liu, W. Zhou and S. Xie: Opt. Mater. Express **2** (2012) 839.
39 M. E. Itkis, S. Niyogi, M. E. Meng, M. A. Hamon, H. Hu and R. C. Haddon: Nano Lett. **2** (2002) 155.
40 M. E. Itkis, F. Borondics, A. Yu and R. C. Haddon: Science **312** (2006) 413.
41 X. Dai, S. Zhang, Z. Wang, G. Adamo, H. Liu, Y. Huang, C. Couteau and C. Soci: Nano Lett. **14** (2014) 2688.
42 A. M. Munshi, D. L. Dheeraj, V. T. Fauske, D. C. Kim, A. T. J. van Helvoort, B. Fimland and H. Weman: Nano Lett. **12** (2012) 4570.
43 Y. J. Hong, W. H. Lee, Y. Wu, R. S. Ruoff and T. Fukui: Nano Lett. **12** (2012) 1431.
44 L. Sang, M. Liao and M. Sumiya: Sensors **13** (2013) 10482.
45 S. C. Jain, J. Narayan and R. V. Overstraeten: J. Appl. Phys. **87** (2000) 965.
46 J. G. Lu, P. Chang and Z. Fan: Mater. Sci. Eng. **52** (2006) 49.
47 T. Zhai, Z. Fang, M. Liao, X. Xu, H. Zeng, B. Yoshio and D. Golberg: Sensors **9** (2009) 6504.
48 H. Kind, H. Yan, B. Messer, M. Law and P. Yang: Adv. Mater. **14** (2002) 158.
49 Z. Li, R. Yang, M. Yu, F. Bai, C. Li and Z. L. Wang: J. Phys. Chem. C **112** (2008) 20114.
50 R. R. Nair, P. Blake, A. N. Grigorenko, K. S. Novoselov, T. J. Booth, T. Stauber, N. M. R. Peres and A. K. Geim: Science **6** (2008) 1308.
51 T. J. Echtermeyer, L. Britnell, P. K. Jasnos, A. Lombardo, R. V. Gorbachev, A. N. Grigorenko, A. K. Geim, A. C. Ferrari and K. S. Novoselov: Nat. Commun. **2** (2011) 458.
52 Y. Liu, R. Cheng, L. Liao, H. Zhou, J. Bai, G. Liu, L. Liu, Y. Huang and X. Duan: Nat. Commun. **2** (2011) 579.
53 E. D. Minot: Tuning the Band Structure of Carbon Nanotubes, A Dissertation Presented to the Faculty of the Graduate School of Cornell University (2004).
54 Z. Liu, T. Luo, B. Liang, G. Chen, G. Yu, X. Xie, D. Chen and G. Shen: Nano Res. **6** (2013) 775.
55 W. Y. Weng, T. J. Hsueh, S. J. Chang, S. B. Wang, H. T. Hsueh and G. J. Huang: IEEE J. Sel. Top. Quantum Electron. **17** (2011) 996.
56 D. Shao, M. Yu, H. Sun, T. Hu, J. Lian and S. Sawyer: Nanoscale **5** (2013) 3664.